

Lawrence Berkeley National Laboratory

Recent Work

Title

MICROSTRUCTURAL INFLUENCE ON ABRASIVE WEAR RESISTANCE OF HIGH STRENGTH, HIGH TOUGHNESS MEDIUM CARBON STEELS

Permalink

<https://escholarship.org/uc/item/6r93r5h7>

Authors

Kwok, C.K.
Thomas, G.

Publication Date

1982-09-01

c.2



Lawrence Berkeley Laboratory

UNIVERSITY OF CALIFORNIA

RECEIVED
LAWRENCE
BERKELEY LABORATORY
OCT 27 1982
LIBRARY AND
DOCUMENTS SECTION

Materials & Molecular Research Division

To be presented at the Wear Conference 1983,
Reston, VA, April 11-14, 1983

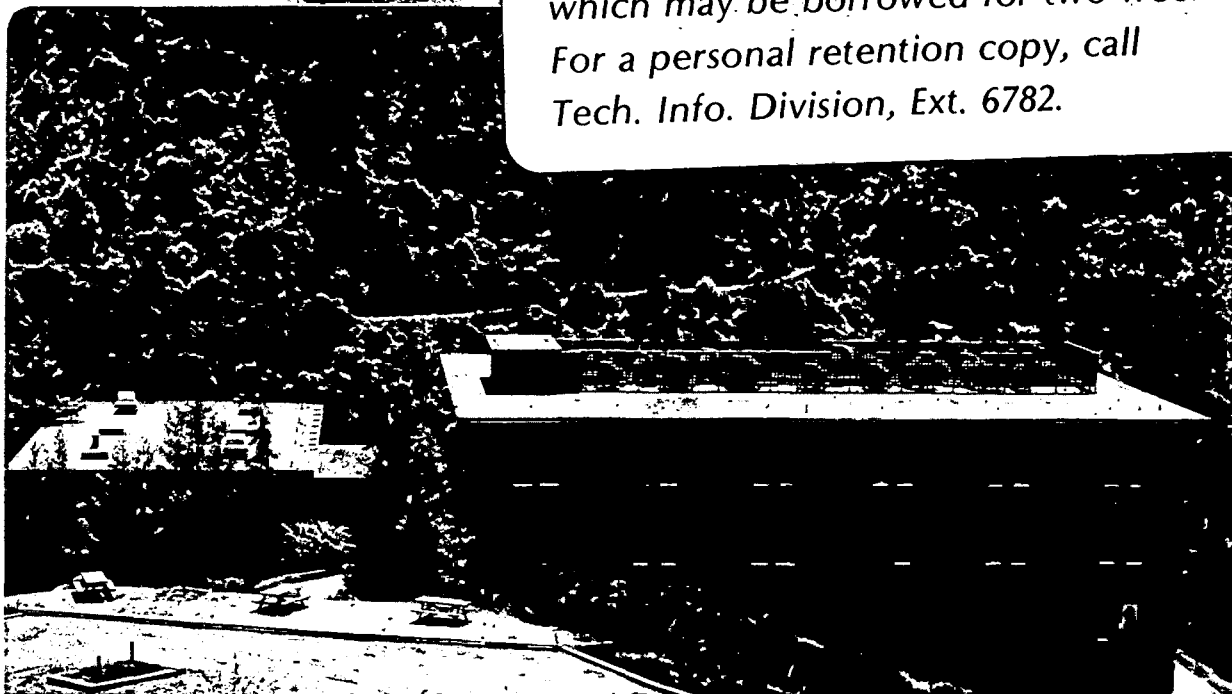
MICROSTRUCTURAL INFLUENCE ON ABRASIVE WEAR
RESISTANCE OF HIGH STRENGTH, HIGH TOUGHNESS
MEDIUM CARBON STEELS

C.K. Kwok and G. Thomas

September 1982

TWO-WEEK LOAN COPY

*This is a Library Circulating Copy
which may be borrowed for two weeks.
For a personal retention copy, call
Tech. Info. Division, Ext. 6782.*



LBL-14911
c.2

DISCLAIMER

This document was prepared as an account of work sponsored by the United States Government. While this document is believed to contain correct information, neither the United States Government nor any agency thereof, nor the Regents of the University of California, nor any of their employees, makes any warranty, express or implied, or assumes any legal responsibility for the accuracy, completeness, or usefulness of any information, apparatus, product, or process disclosed, or represents that its use would not infringe privately owned rights. Reference herein to any specific commercial product, process, or service by its trade name, trademark, manufacturer, or otherwise, does not necessarily constitute or imply its endorsement, recommendation, or favoring by the United States Government or any agency thereof, or the Regents of the University of California. The views and opinions of authors expressed herein do not necessarily state or reflect those of the United States Government or any agency thereof or the Regents of the University of California.

Microstructural Influence on Abrasive Wear Resistance of
High Strength, High Toughness Medium Carbon Steels

C.K. Kwok and G. Thomas

Department of Materials Science and Mineral Engineering and the
Lawrence Berkeley Laboratory
University of California
Berkeley, California 94720

A systematic study of abrasive wear resistance of Fe/Cr/Mn experimental steels has been carried out in two body pin-on-disc abrasion tests. Silicon carbide, alumina and quartz were used as abrasives. The relationships between microstructures, mechanical properties and abrasive wear resistance for these experimental steels were studied. In addition, several commercial alloys were tested to provide a basis for comparison. Results show that dislocated lath martensite with continuous interlath films of retained austenite appears to be a desirable microstructure for good wear resistance. Grain refinement by double heat treatment was found to improve the toughness in the experimental steels but have little effect on the abrasive wear resistance. In general, superior tensile properties and wear resistance, without sacrifice in toughness, can be achieved by a lath martensitic microstructure.

INTRODUCTION

In ferrous alloys the optimum combination of mechanical properties can be achieved by careful control of their microstructures through proper alloy additions and thermal mechanical treatments. Most wear applications, such as mineral mining and processing activities, demand a class of alloy which is both tough and wear resistant. Toughness, as well as abrasive

*presented at the Wear Conference 1983, Virginia, April 1983.

wear resistance is equally important since many processing operations involve continuous impact and wear. Failure can occur either when the part breaks through impact or is worn to a point where it can no longer function properly.

In recent years, a program¹⁻⁴ has been systematically carried out at Berkeley to investigate the effect of alloying elements and heat treatment on the martensitic microstructure of a group of ternary Fe/Cr/C and quaternary Fe/Cr/Mn/C alloys.

These experimental alloys have superior tensile strength and toughness as compared to many commercial alloys. In addition, a recent study⁷ has also shown that their sliding wear resistance is greater than many commercial wear-resistant alloys. Since many wear problems involve two body and three body abrasion, it is important therefore to understand the abrasive wear characteristics of these steels and their responses to thermal treatment.

II. EXPERIMENTAL PROCEDURES

A. Alloy Preparation and Heat Treatment

1) Experimental Alloys. The composition of the experimental alloys (designated Quatough steels) and commercial alloys are listed in Table 1. The Quatough alloys, designed for high strength and toughness⁴ were melted by Daido Steel Co., Japan. The vacuum-induction melts were cast into 10Kg ingots and subsequently forged to 2.54cm thick and 6.35cm wide slabs. Then, they were homogenized at 1200°C for 24 hours and furnace cooled.

Three different heat treatments were applied to the experimental alloys, namely HT(I), (II) and (III) are shown diagrammatically in Fig.

1. Their relative merits will be discussed in a later section. Basically,

the heat treatment involved high temperature austenitizing (1100°C), oil quenching and subsequent tempering. HT (III) and HT (II) require a second low temperature austenitizing (870°C) and subsequent quenching and tempering with or without an intermediate 200°C tempering, respectively. All the austenitizing treatments were carried out in a vertical tube furnace under an inert gas atmosphere. At the end of the austenitization, specimens were quenched into agitated oil. All tempering treatments (200°C to 500°C) were performed by immersing the specimens into a salt pot for one hour and then quenching into cold water.

2) Commercial alloys. All commercial alloys, namely, alloy A, B and C were used in as-received conditions. AISI 1020 was purchased and used in a hot-rolled condition.

B. Metallography

1) Optical metallography. Specimens for optical metallography were cut from heat-treated material, mounted in cold mount resin, abraded on silicon carbide paper down to 600 grit, and then polished with 1 μ m diamond paste on a microcloth. A 5% nital etchant was used to reveal the microstructures.

2) Transmission Electron Microscopy. Thin foils of \sim 500 μ m thickness were cut from the heat-treated alloys via a Diamet saw. These slices were then chemically thinned to 125 μ m in a 4% solution of HF in H₂O₂. 3.0mm discs were obtained by spark cutting and were abraded down to 25-50 μ m thickness by 400/600 grit abrasive paper. Final polishing was achieved using a twin-jet electropolisher at room temperature, with a solution of 75g of CrO₃, 400ml CH₃COOH and 21ml distilled water. The polishing voltage was 40-45 volts at 50-55 milliamps. Once suitable

thin foils were produced, transmission electron microscopy was carried out, using either a JEM7A or a Philips 301 electron microscope, both operating at 100kV.

C. Wear Properties

1) Wear specimen preparation. Wear pins were cut from the heat-treated specimens in the form of rectangular bars. Then they were machined to 6.35mm in diameter by 20mm long hemispherically-tipped cylindrical pins. The tips were ground to exact size under flood cooling to prevent any heat-induced microstructural change.

The specimens were hand-cleaned in N-heptane to remove oil and dirt, and then ultrasonically cleaned by ethyl alcohol for 5 minutes before finally being placed in a vacuum desiccator to remove any moisture left on the surface.

The specimens were weighed prior to each wear test on a Mettler H54AR analytical balance to an accuracy of $\pm 0.01\text{mg}$. Three measurements were taken for each pin and the median value recorded. After every wear test, the wear pins were carefully dusted off by a gentle stream of compressed helium gas and reweighed. The weight loss was then determined and converted to wear resistance as shown below:

$$\begin{aligned}\text{Wear resistance} &= 1/\text{wear rate} \\ &= \frac{\text{length of wear path}}{\text{volume of material removed}} \\ &= \frac{(\text{material density}) (\text{length of wear path})}{\text{weight loss}} \text{mm/mm}^3\end{aligned}$$

2) Wear test. The two-body, dry abrasive wear tests were performed on a pin-on-disc wear machine which simulated high stress abrasion. The wear pins were worn against abrasive paper for 10 revolutions at a

rotational speed of 20rpm under 1 kg deadweight load. A spiral wear track, about 2.2 meters in length, was generated as the wear pin moved transversely across the abrasives. A spiral path was used to ensure that unworn abrasives were encountered on each revolution. The worn specimens were lifted off automatically by a mechanical relay after 10 revolutions.

A break-in run was carried out prior to each of the three wear tests performed on each pin. The subsequent weight losses were measured and a mean value was calculated. Two pins were tested for each material, using the same experimental conditions. Finally, the two mean values for weight loss were combined and converted to a value of wear resistance, to generate one datum point. The experimental data were found to be quite reproducible giving only a 3-5% scatter band.

Three abrasives, 120 grit SiC, 120 grit carborundum Al_2O_3 , and 40 grit flint SiO_2 were used in the wear test to assess the effect of abrasive geometry and hardness on abrasive wear.

III. RESULTS

A. Optical Metallography

Optical metallography was performed to confirm the microstructure and prior austenite grain size of the experimental material used in the wear tests. The experimental alloys were found to be composed of uniform packets of lath martensite, with no dissolved carbides observed. Double heat-treatments (II) and (III) decreased the grain diameter by an order of magnitude (from 270 to 30 microns) in comparison to the conventional heat treatment (I), (see Figure 2).

The commercial wear-resistant alloys A, B and C all had a martensitic and/or bainitic microstructure. In addition, elongated MnS inclusions were

observed in the C alloy (see Figs. 3(a), (b), (c)). The AISI 1020 alloy was found to have a pearlitic/ferritic microstructure, an example of which is shown in Figure 3(d).

B. Transmission Electron Microscopy

1) Experimental alloys. In recent years the TEM microstructures of Fe/3Cr/2Mn/0.5Mo/.3C alloys have been well-documented⁵ through TEM. The as-quenched microstructure was found to be a highly-dislocated lath martensite with continuous interlath films of retained austenite. The typical lath dimensions were about 0.5 microns in width and 5-10 microns in length (Figure 4 and 5).

Upon 200°C tempering, $\langle 110 \rangle_{\alpha}$ Widmanstätten cementite precipitates were observed within the martensite laths and were typically 0.3 - 0.5 μm long and 200Å to 500Å wide. At 300°C tempering, cementite precipitation was observed both within the lath and at the lath boundaries (Figure 5). At 400°C and 500°C tempering, extensive carbide precipitation inside the laths, and discontinuous stringers of carbide at lath boundaries were observed. Spheroidization appeared to have started at 400°C and continued at 500°C tempering.

TEM studies of double heat-treated specimens showed a similar transformation with tempered martensite embrittlement beginning at 300°C. The martensite packet size was smaller in comparison to conventional heat-treated specimen, but the lath width was relatively unchanged.

2) Commercial alloys. Interlath and intralath carbides were observed in alloy A, a consequence of the bainitic structure. Alloy B however, appeared to have a complex martensitic microstructure with a small amount of microtwins present, whereas alloy C was found to have a

non-uniform bainitic/martensitic microstructure in which extensive carbide precipitation was observed¹⁷.

Although the above commercial alloys had microstructures similar to those observed in the experimental alloys, there were important differences that resulted in the greater toughness of the latter viz. the uniformity of martensite packets and the presence of continuous interlath films of retained austenite.

C. Mechanical properties. A summary of the mechanical properties of the experimental alloys is shown in Table 2 and Figure 7. The ultimate tensile strength, yield strength, Charpy toughness and hardness curves all show a similar tempering response in that they all increase slightly from the as-quenched condition to 200°C tempering, then decrease drastically after 300°C, and continue to decrease at 400°C and 500°C tempering. This abrupt decrease in Charpy toughness is mainly due to tempered martensite embrittlement (TME), caused by the transformation of interlath austenite to deleterious interlath carbide stringers at temperatures greater than 300°C⁶.

Some of the mechanical properties of the commercial alloys were provided by their respective manufacturers (see Table 2).

D. Wear Test. Wear tests were performed on a 2-body pin-on-disc wear machine, and a summary of the wear data is shown in Table 3.

Three abrasives were used in the tests and their cutting efficiency in wear can be ranked in the following order starting with the most efficient: Al₂O₃, SiC and SiO₂. Even though Al₂O₃ is softer than SiC the wear rate of all alloys against Al₂O₃ was higher mainly because Al₂O₃ had a better bond-adherence between the abrasives and the supporting media.

The wear resistance of vacuum-melted Fe/3Cr/2Mn/.5Mo/.3C steel was found to be superior to alloy A, B, C and AISI 1020 and generally was 20-40% higher than these commercial alloys. The wear resistance was also measured as a function of tempering temperature for the experimental alloys and compared to the equivalent plots for impact toughness, tensile strength, yield strength and hardness (see Figures 7 and 8). The effect of tempering temperature on the wear resistance is effectively the same for the as-quenched and the 200°C tempered state. However, the wear resistance dropped abruptly after tempering at 300°C, only to gradually increase again (by a total of ~5%) after 400°C and 500°C tempering.

When SiC was used in the wear tests, there was little difference in wear resistance between the double heat-treated and the conventional single heat-treated specimens. However, when quartz (SiO₂) was used, there was some (see Table 3) measureable improvement observed in the grain-refined specimen. When the commercial alloys were tested with each of the three different abrasives, Alloy A, B and C all had similar wear rates. As Alloy B had a higher ultimate tensile strength (UTS) and hardness than Alloy A and C, it is interesting to note that alloy B did not have a better wear resistance than the other two commercial alloys.

IV. DISCUSSION

1) Effect of tempering on abrasive wear. There are three principal ways of strengthening the structure of steels: (a) alloying, (b) work hardening, and (c) heat treating.

(a) For most ferrous alloys, an increase in carbon content is the most effective way to increase wear resistance. Hardenability, bulk hardness and volume fraction of alloy and iron carbides, are all believed

to be beneficial to abrasive wear resistance, and all increase with increasing carbon content. Previous studies^{4,5} have shown the micro-structural twinning occurs when the carbon content of experimental alloys is equal or greater than 0.3%. Therefore, this posts an upper limit upon the carbon content of 0.3%, as twinned martensite is known to possess more inferior fracture and impact toughness properties than lath martensite. The addition of chromium to steel improves both strength and toughness and has a small but measurable effect in improving abrasive wear⁷. However, if 0.5% molybdenum is added and chromium reduced by 1%, no detrimental effect upon either the high strength or the high toughness of the quaternary alloy occurs⁵. Moreover, molybdenum may reduce the severity of temper embrittlement⁸. The final composition of Fe/3Cr/2Mn/0.5Mo/.3C gives optimum strength and wear properties without any sacrifice in toughness.

(b) Extensive work-hardening in the form of plowing always occurs during abrasive wear, so there is little profit in improving bulk hardness through prior cold-working. Thus, the wear resistance is relatively independent of prior cold work^{9,10}.

(c) It is likely that improving the strength of the material through heat treatment will produce a corresponding increase in wear resistance. In the present experiment, Quatough steels have been subjected to different tempering conditions (from as-quenched to 500°C tempering) after high temperature austenitization and oil quenching. Comparisons between wear resistance and hardness, tensile strength and yield strength show a similar trend (See Figures 7 and 8). The wear resistance of the experimental alloys in the as-quenched state and 200°C tempered state are about equal but decrease abruptly at 300°C tempering. At 400°C and 500°C

tempering, wear resistance is gradually increased by a total of 5%. The sharp decrease in both fracture toughness and wear resistance after 300°C is a direct result of the onset of tempered martensite embrittlement. At this stage in tempering, the continuous films of interlath, retained austenite transform to iron carbides. It is likely that these carbides limit the plastic zone in front of any intralath crack to the width of the martensite lath, and thus promote unstable crack propagation.

At higher tempering temperatures, carbides continue to grow and eventually spheroidize. A decrease in the stress concentration at the site of tempered carbides (due to spheroidization) decreases the tendency of crack initiation at those Widmanstätten intralath carbides and easy crack-propagation through interlath carbides.

Ultimate strength, yield strength and hardness tempering curves all have a similar slope (up to 300°C tempering) to that of the wear resistance curve of the experimental alloy (Figure 7). When the same material is considered with different mechanical properties through different heat treating conditions, UTS, YS and hardness and its wear resistance are correlated to each other. However, when different materials are compared, data points become more scattered. This occurs because wear rate is microstructurally sensitive so different microstructures (e.g. martensitic, bainitic, pearlitic, or ferritic) respond differently during abrasive wear.

Although the microstructures of the commercial alloys and the experimental alloys appear to be somewhat similar (martensitic or martensitic/bainitic complex), the inferior wear properties of commercial steels, may be due to their nonuniform distribution of large carbides

and/or interlath carbide formation.

The effect of retained austenite on abrasive wear has been shown to be beneficial by many investigations³⁷⁻⁴⁰. The enhancement of wear resistance by the retained austenite may be due to (i) the transformation induced plasticity (TRIP) that can absorb energy for fracture and produce local compressive stresses that impede microcrack formation; (ii) the presence of the ductile austenite film between the martensite laths discouraging microcrack nucleation and propagation. Previous evidence¹⁵ has shown that crack propagation through a retained austenite phase was arrested; (iii) an increase in work-hardening coefficient through TRIP or (iv) retention of retained austenite at lath boundary preventing brittle lath boundary carbide formation. In the case of the Quatough steels, the amount of retained austenite determined by X-ray diffractometry is about 2% in the as-quenched condition, decreasing abruptly to zero percent at or above 300°C tempering temperature. Because the experimental error involved in detecting retained austenite by X-ray diffractometry is typically >0.5%, it is difficult to establish any quantitative correlation between the amount of retained austenite and the wear resistance.

Mössbauer spectroscopy has been performed on both the experimental and commercial alloys to determine the volume fraction of retained austenite quantitatively¹⁶. The amount of retained austenite in the following steels -- Quatough, Alloy A, B and C -- is 3.5%, 0.3%, 1.5% and 5%, respectively¹⁷. Again no conclusive, quantitative relationship between the amount of retained austenite and abrasive wear resistance is possible. The data in Table 3 show that although the commercial alloys have a

different volume fraction of retained austenite, their wear resistance is almost identical. Nevertheless, in the case of low carbon, structural steels, the distribution and morphology of retained austenite (interlath, intralath, thin, continuous film vs. block) may be more important than the relative amount present.

3) Effect of grain-refinement on abrasive wear. For most ferrous alloy systems, it is generally true that the flow stress is inversely proportional to the square root of grain diameter^{18,19}. Any heat treatment that refines the grain should improve the strength. Since hardness and ultimate tensile strength are well known for their beneficial role in abrasive wear²⁰, grain-refinement is one possible way to improve abrasive wear resistance.

Previous experiments⁴ have shown that the fracture and impact toughness of experimental alloys were significantly improved by austenitizing at a higher temperature (1100°C). This allows for dissolution of the alloy carbides. However, the prior austenite grains were relatively coarse ($\sim 270\mu\text{m}$ with HT (I)). Grain-refinement can be achieved by re-austenitizing the Quatough alloys at 870°C. This results in reducing the prior austenite grain diameters to $\sim 35\mu\text{m}$ and $30\mu\text{m}$ with HT (II) and HT (III), respectively.

From the results shown in Tables 2 and 3, the wear resistance, hardness, UTS and YS of the Quatough steel is relatively constant whereas fracture toughness and impact toughness increase moderately when subjected to double heat-treatment. Neither the tensile properties nor the wear resistance obey the classical Hall-Petch inverse square root relationship. However, they are in agreement with each other.

This apparent discrepancy, in which the prior austenite grain diameter decreases an order of magnitude with little corresponding change in both tensile properties and wear resistance, can possibly be explained by either (i) the martensite lath size, which does not noticeably change under HT (II) and HT (III), and is a more fundamental parameter controlling the mechanical properties; most microcracks initiate either at an inclusion or a cracked cementite particle within the martensite lath, and they tend to propagate through the laths along their longitudinal lath axis in a zig-zag fashion, as laths change orientation from one packet to another. The nominal lath length is 5-10 μ m, so they are much smaller than prior austenite grain size, the lath boundaries become effective barrier of crack propagation, or (ii) the high dislocation density due to the rapid oil quench; the movement of dislocation is limited to very short distance before impingement occurs. A prior austenite grain diameter of 30 μ m with HT (III) is too large to be an effective dislocation barrier.

The main benefit of double heat treatment is improving fracture toughness by a fine redistribution of the interlath iron carbides in the matrix, and also increase the amount of retained austenite slightly in the alloy.

V. CONCLUSION

1) The best abrasive wear resistance of Fe/3Cr/2Mn/.5Mo/.3C is obtained in the as-quenched condition. However, a 200°C tempering gives optimum tensile and fracture toughness properties without an appreciable decrease in the wear resistance.

2) The wear resistance decreases sharply after 300°C tempering

and is likely due to the transformation of interlath retained austenite to carbides.

3) Highly dislocated lath martensite with continuous film of retained austenite appears to be a preferable microstructure than either a bainitic/martensitic or a ferritic/pearlitic microstructure for good wear resistance.

4) Grain-refinement by double heat treatment improves the toughness but appears to have little effect on the abrasive wear resistance.

VI. ACKNOWLEDGEMENTS

The authors wish to thank Dr. William Salesky and Dr. Judy Rayment for their helpful discussions.

This work was supported by the Director, Office of Energy Research, Office of Basic Energy Sciences, Materials Sciences Division of the U.S. Department of Energy under Contract No. DE-AC03-76SF00098.

REFERENCES

1. G. Thomas, Met. Trans. 2, 2373 (1972).
2. J. McMahon and G. Thomas, Proc. 3rd International Conference on Strength of Metals and Alloys, Inst. of Metals, London 1, 180 (1973).
3. B.V.N. Rao and G. Thomas, Mat. Sci. and Eng. 20, 198 (1975).
4. B.V.N. Rao and G. Thomas, Met. Trans. A11, 411 (1980).
5. M. Sarikaya, M.S. Thesis, University of California, Berkeley, June 1979, LBL #9260.
6. G. Thomas, Met. Trans. 9A, 439 (1978).
7. R.A. Garriga, M.S. Thesis, University of California, Berkeley, August 1979.
8. S.K. Bannerjee, C.J. McMahon Jr., and H.C. Feng, Met. Trans. 9A, 237 (1978).
9. M.M. Khrushov and M.A. Babichev, Friction and Wear in Machinery 19, 1 (1965).
10. K.H.R. Wright, Tribology 2 (3), 152 (1969).
11. M.S. Bhat, V.F. Zackay and E.R. Parker, Proc. of 3rd. Conference on Material for Coal Conversion and Utilization, October 1978.
12. N.J. Kar, Wear of Material 1981, p. 415.
13. K.H. Zurn Gahr, Metal Progress, September 1979, 46.
14. P.L. Hurrick, Wear 26, 285 (1973).
15. D. Webster, Trans. A.S.M. 61, 816 (1968).
16. B. Fultz, M.S. Thesis, University of California, Berkeley, June 1978, LBL #7671.
17. W.J. Salesky and G. Thomas, Wear 75, 21 (1980).

18. E.O. Hall, Proc. Phys. Soc. Series B 64, 747 (1951).
19. N.J. Petch, J. Iron Steel Inst. 174, 25 (1953).
20. M.A. Moore, Wear 27, 1 (1974).

FIGURE CAPTIONS

- Fig. 1. Illustration of heat treatments employed in this study.
- Fig. 2. Optical micrographs of experimental steel: (a), (b), and (c) are from HT(I), (II), and (III), respectively.
- Fig. 3. Optical micrographs of commercial alloys (a) alloy C, (b) alloy A, (c) alloy B, and (d) AISI 1020.
- Fig. 4. TEM micrographs of Quatough experimental alloys (a)HT(I), (b)HT (III).
- Fig. 5. Bright field (a) and dark field (b) micrographs showing retained austenite phase in Quatough experimental alloy following HT (II) in the 200°C tempered condition.
- Fig. 6. Bright field (a) and dark field (b) of 300°C tempered Quatough experimental alloy. Note extensive twin carbide precipitation.
- Fig. 7. Wear resistance and mechanical properties versus tempering temperature showing that tempering martensite embrittlement (occurring at ~300°C) leads to an abrupt drop in wear resistance.
- Fig. 8. Wear resistance of experimental steel run on three different abrasives showing similar tempering responses.

TABLE 1

Steel Composition

	C	Cr	Mn	Ni	Mo	Co	Si	Ti	V	Fe
QUATOUGH	0.26	3.11	1.98	0.01	0.50	-	-	-	-	Bal.
Alloy A	0.35	0.45	0.87	0.58	0.14	-	0.20	-	-	Bal.
Alloy B	0.29	1.67	1.07	3.68	0.37	0.08	0.42	0.007	0.01	Bal.
Alloy C	0.26	0.30	1.94	0.73	0.24	-	0.57	0.06	-	Bal.
AISI 1020HR	0.20	-	0.45	-	-	-	-	-	-	Bal.

TABLE 2

Mechanical Properties

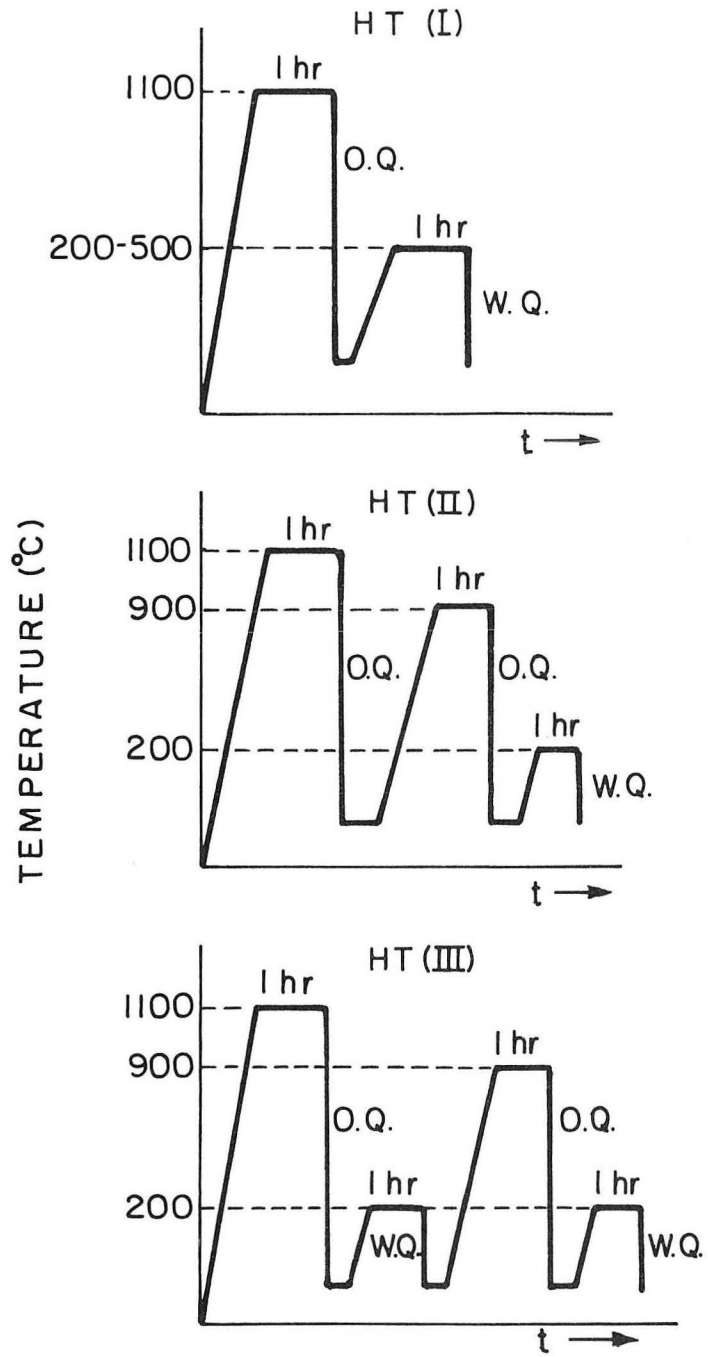
Alloy	Tempering (Temp. (°C))	UTS (MPa)	YS (MPa)	Total Elongation(%)	Charpy Toughness(J)	Fracture Toughness(MPa-m) ^{1/2}	Hardness (Rc)
Fe/3Cr/2Mn/0.5Mo/ 0.3C HT(I)	AQ	1744	1379	6.25	39.0	88	48.5
	200	1772	1413	7.0	47.0	121.6	48
	300	1420	1220	8.0	30.5		45
	400	1379	1172	8.1	30.0		42
	500	1338	1145	7.0	27.0		40.5
	HT(II) 200	1724	1320	11.6	51.5	127.2	48
	HT(III) 200	1724	1338	12.0	57.0	130.0	47
Alloy A		1241	1207	12.0			40
Alloy B		1661	1082	12.0	42.0		45
Alloy C		1365	1269	11.0	20.3		40
AISI 1020HR		448	331	36.0	87.0		110H _B

TABLE 3. Wear Properties

Alloy	Tempering Temp. (°C)	Weight Loss/ Pass(mg) 120 grit SiC	Wear Resistance*	Weight Loss/ Pass(mg) 40 grit SiO ₂	Resistance*	Weight Loss/ Pass(mg) Resistance*		
						120 grit Al ₂ O ₃		
1) Fe/3Cr/2Mn/0.5Mo/0.3C	HT(I)	AQ	1.95	8879	1.61	10754	2.00	8657
2)		200	2.00	8657	1.66	10430	2.21	7843
3)		300	2.38	7275	1.87	9259	2.65	6534
4)		400	2.35	7368	1.87	9259	2.63	6583
5)		500	2.27	7627	1.83	9461	2.57	6737
6)	HT(II)	200	2.06	8405	1.68	10306	-	-
7)	HT(III)	200	2.06	8405	1.56	11100	-	-
8) Alloy A			2.48	6981	1.95	8879	2.89	5991
9) Alloy B			2.40	7214	2.06	8405	2.92	5929
10) Alloy C			2.39	7244	1.99	8701	2.99	5791
11) AISI 1020HR			3.02	5733	2.55	6709	3.45	5019

*(mm/mm³)

HEAT TREATMENTS



XBL 819-6556

Fig. 1

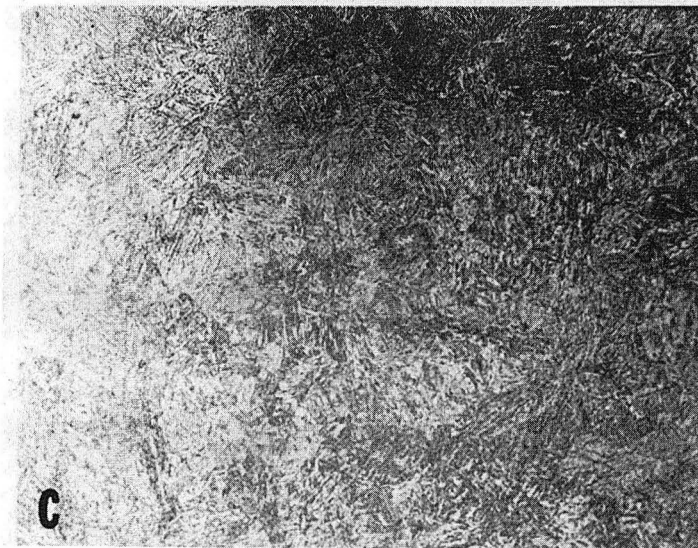
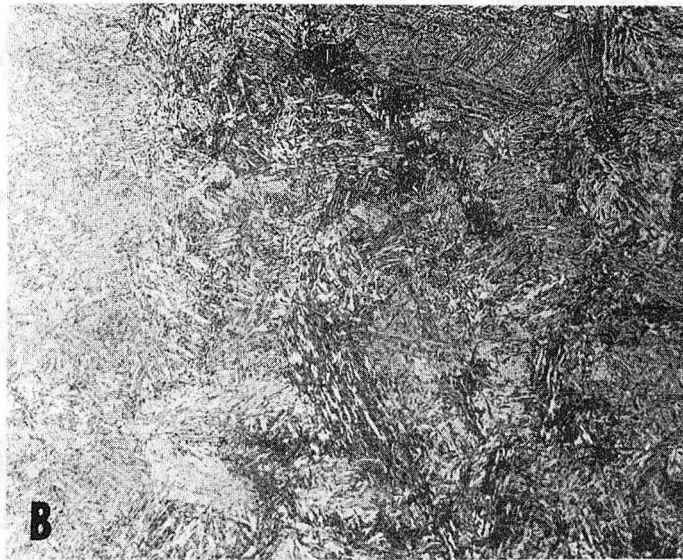
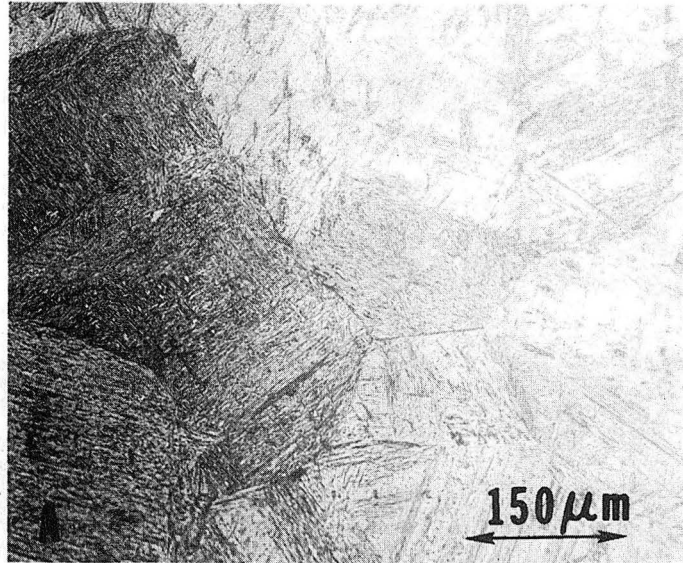


Fig. 2

XBB 810-9825

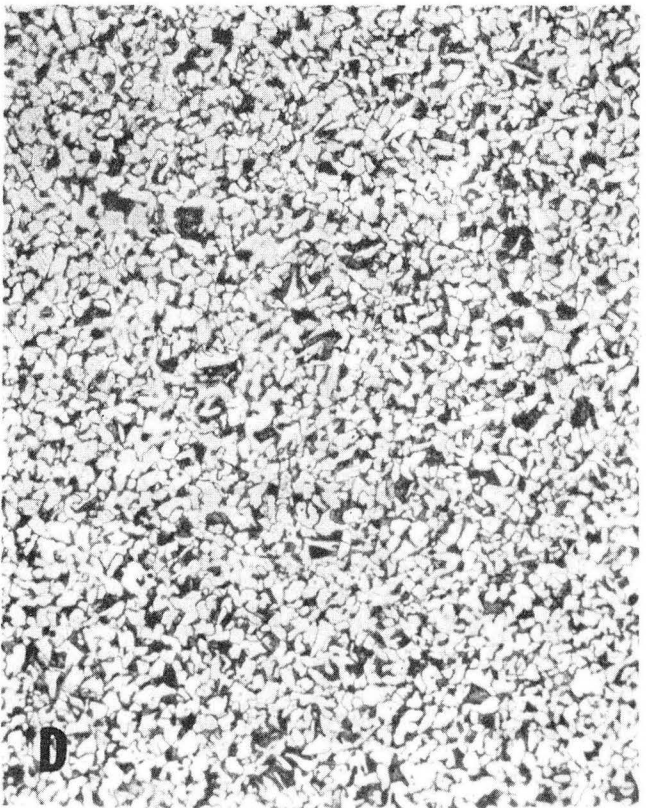
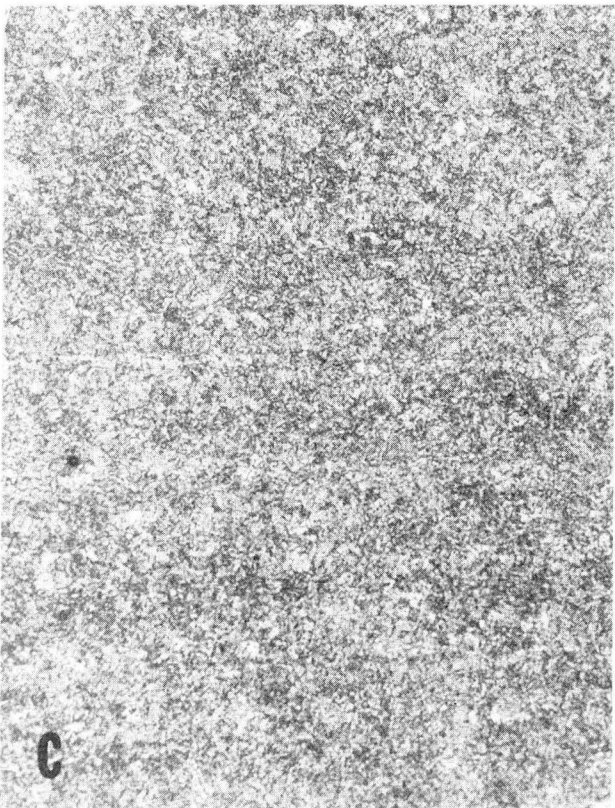
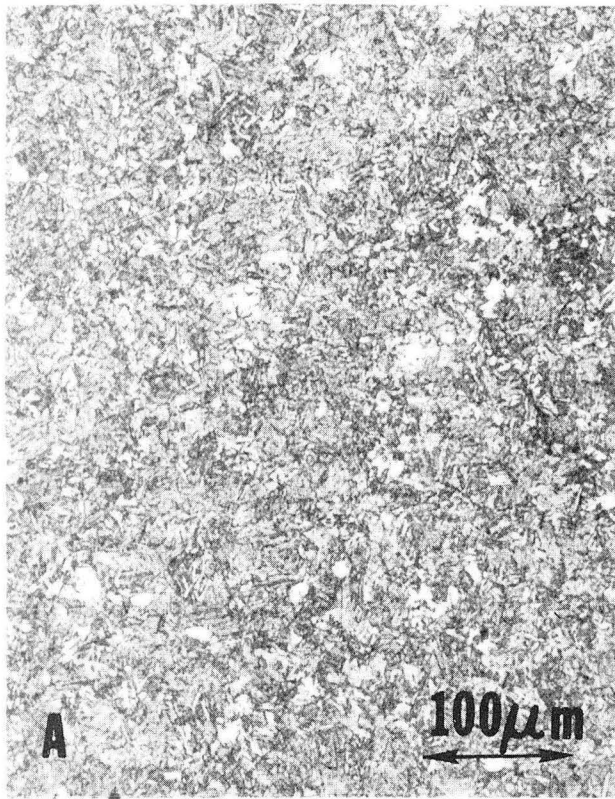


Fig. 3

XBB 810-9832

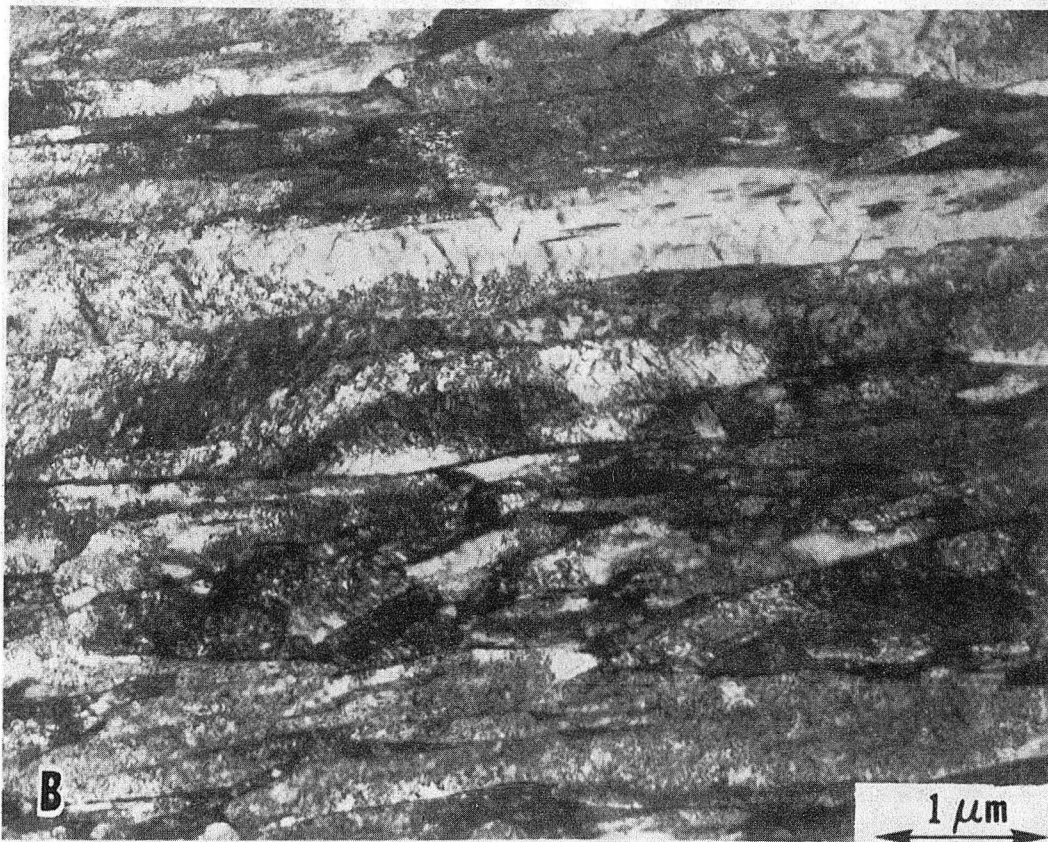
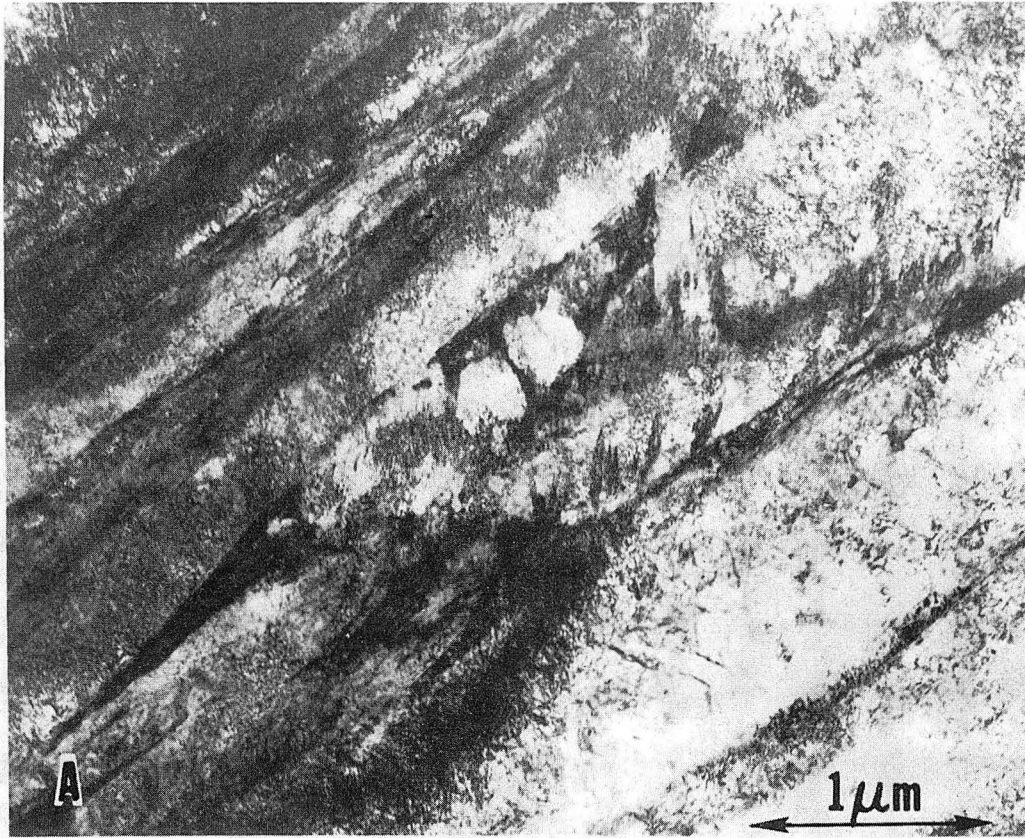
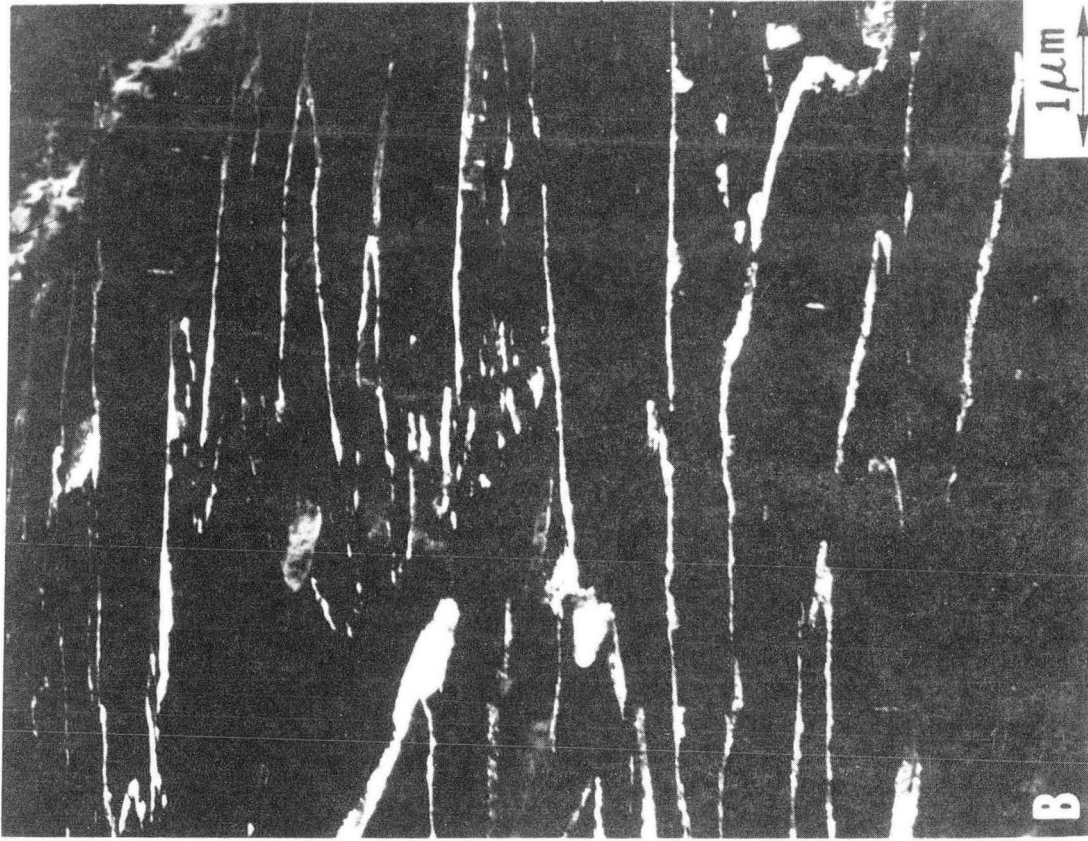


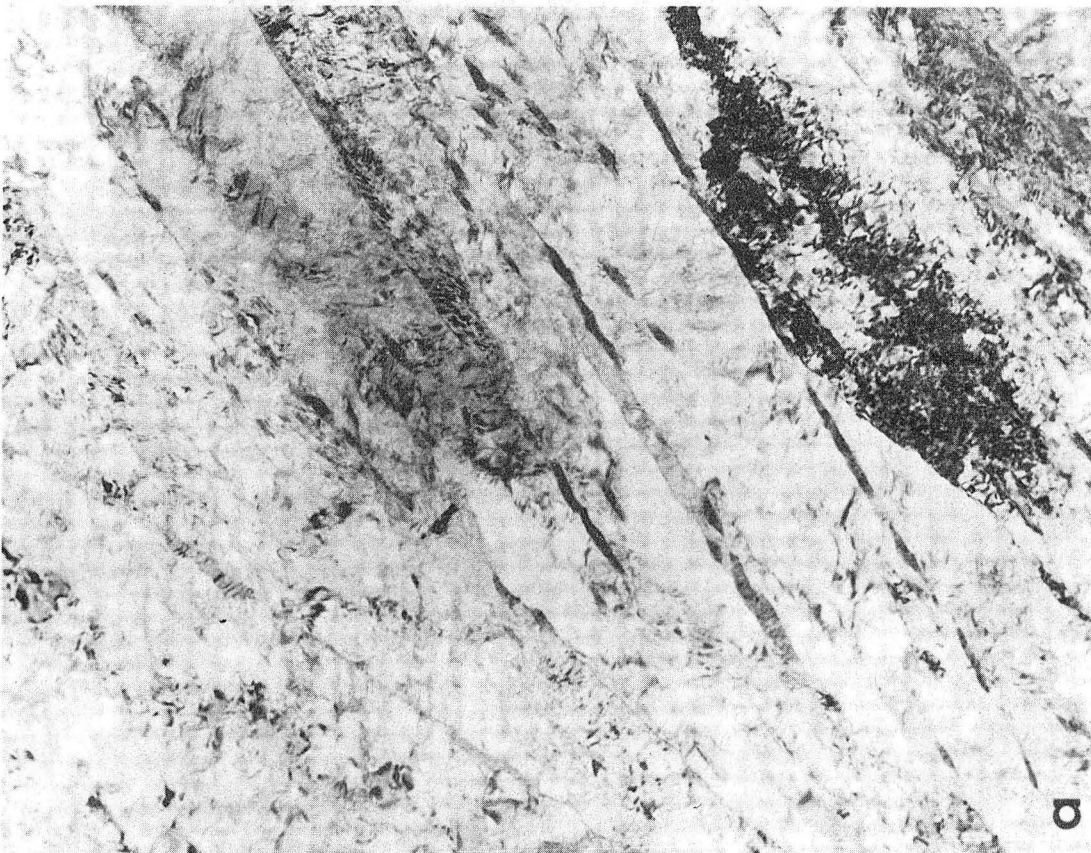
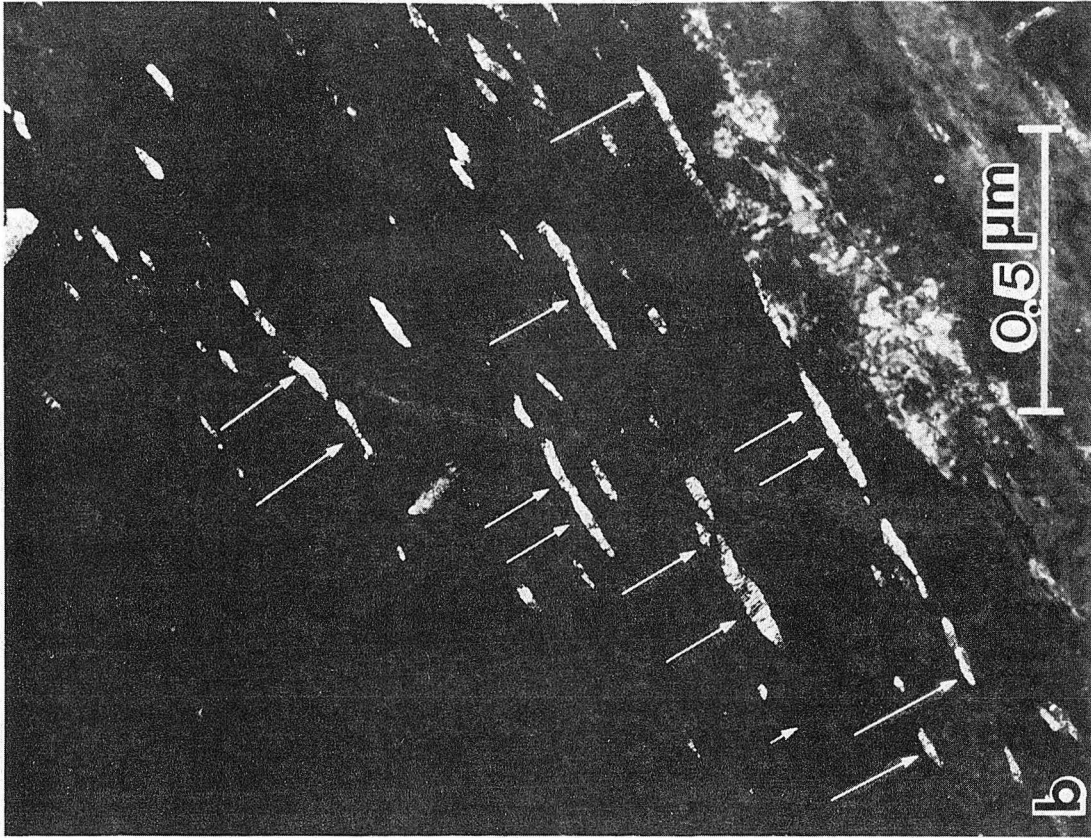
Fig. 4

XBB 810-11084



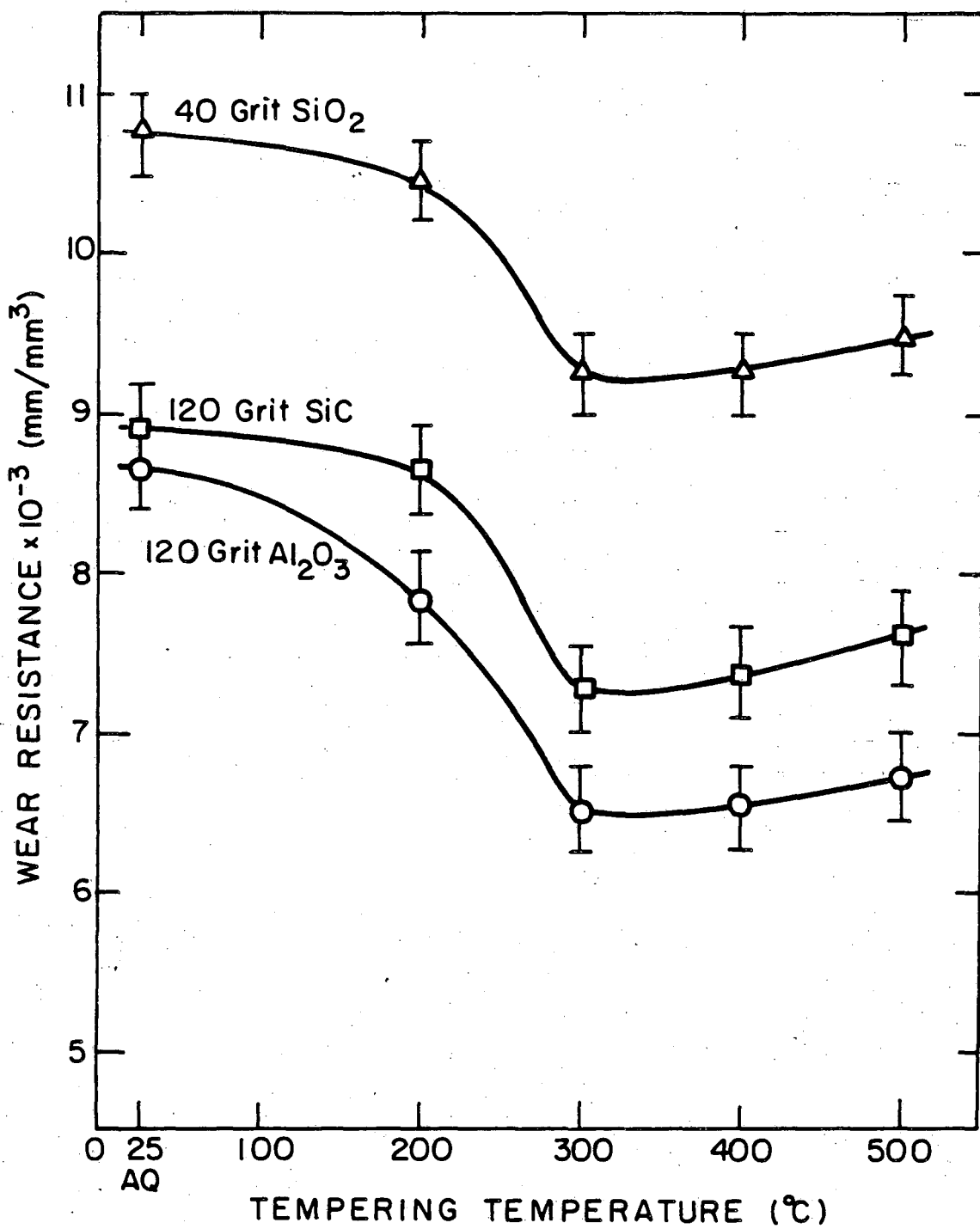
XBB 810-9831

Fig. 5



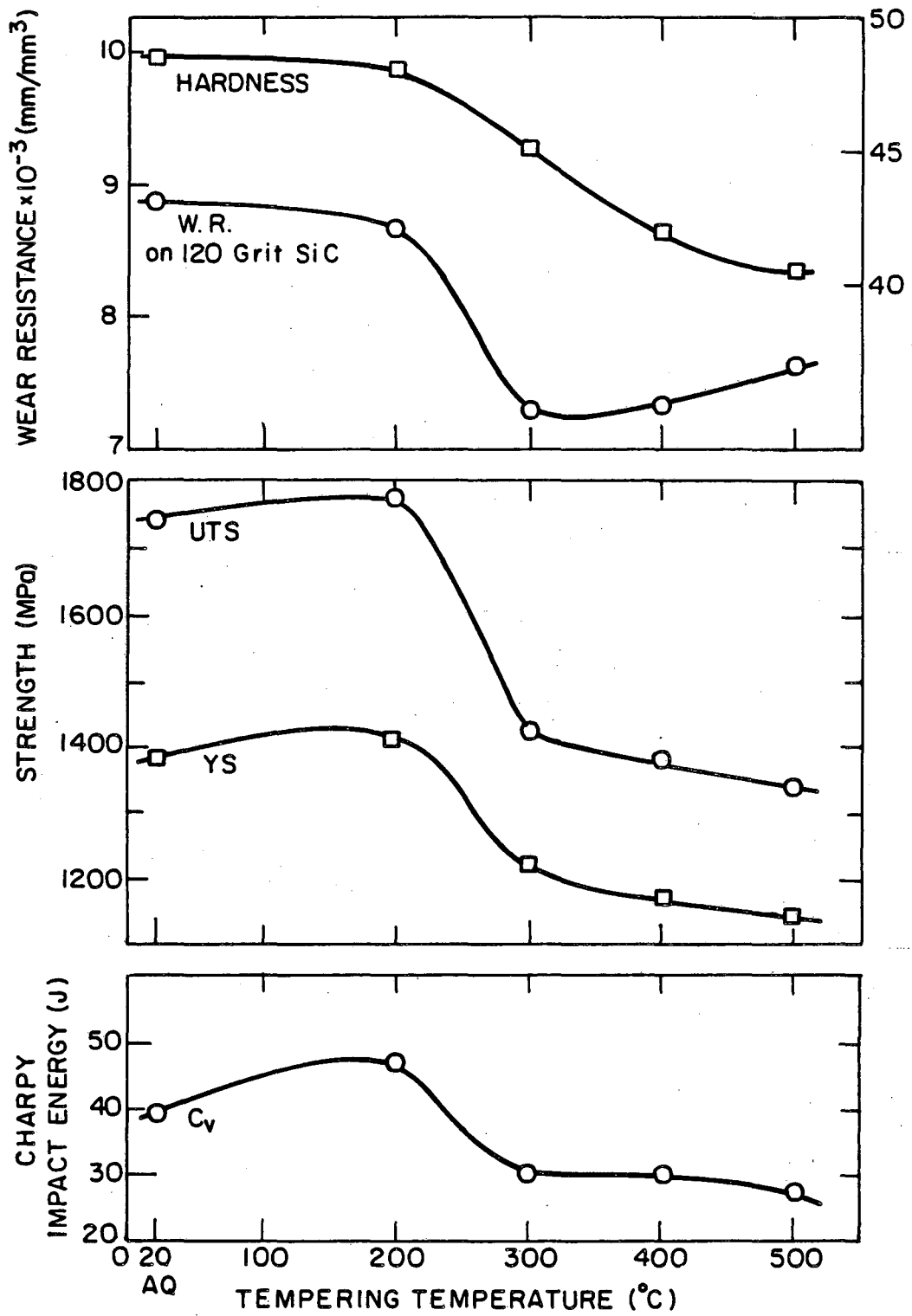
XBB 794-5669

Fig. 6



XBL 819-6554

Fig. 7



XBL 819-6555

Fig. 8

This report was done with support from the Department of Energy. Any conclusions or opinions expressed in this report represent solely those of the author(s) and not necessarily those of The Regents of the University of California, the Lawrence Berkeley Laboratory or the Department of Energy.

Reference to a company or product name does not imply approval or recommendation of the product by the University of California or the U.S. Department of Energy to the exclusion of others that may be suitable.

TECHNICAL INFORMATION DEPARTMENT
LAWRENCE BERKELEY LABORATORY
UNIVERSITY OF CALIFORNIA
BERKELEY, CALIFORNIA 94720